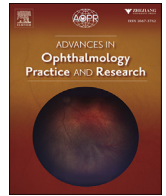




Contents lists available at ScienceDirect

Advances in Ophthalmology Practice and Research

journal homepage: www.journals.elsevier.com/advances-in-ophthalmology-practice-and-research

Review

A comparative study of alteration in retinal layer segmentation alteration by SD-OCT in neuromyelitis optica spectrum disorders: A systematic review and meta-analysis

Junxia Fu^a, Shaoying Tan^b, Chunxia Peng^c, Huanfen Zhou^a, Shihui Wei^{a,*}^a Department of Ophthalmology, The Chinese People's Liberation Army General Hospital & the Chinese People's Liberation Army Medical School, Beijing, China^b School of Optometry, The Hong Kong Polytechnic University, Hong Kong, China^c Department of Ophthalmology, Beijing Children's Hospital, Capital Medical University, National Center for Children's Health, Beijing, China

ARTICLE INFO

Keywords:

Neuromyelitis optica spectrum disorders
Spectral-domain optical coherence tomography
Multiple sclerosis
Idiopathic optic neuritis
Retinal nerve fiber layer

ABSTRACT

Background: To evaluate the feature of different retinal layer segmentation in neuromyelitis optica spectrum disorders (NMOSD) with spectral-domain optical coherence tomography (SD-OCT) and to compare it with that in multiple sclerosis (MS), healthy controls (HC), and idiopathic optic neuritis (ION).

Methods: We retrieved four electronic databases, including Pubmed, Embase, Cochrane Library, and Web of Science from inception to September 1st, 2021. A meta-analysis was performed to compare different retinal layer segmentation thicknesses between patients with or without a history of optic neuritis (ON) in NMOSD and the control group, including patients with MS, HC, and ION.

Results: Forty-two studies were included and the interval between the last ON onset and examination was greater than 3 months. Compared with that in HC eyes, the loss of retinal nerve fiber layer (RNFL) and macular ganglion cell and inner plexiform layer (GC-IPL) was serious in NMOSD eye especially after ON. Moreover, compared with that in ION eyes or MS-related-ON eyes, the injury to the peripapillary retinal nerve fiber layer (pRNFL) was severe in NMOSD-related-ON eyes. In addition, the correlation coefficient between pRNFL and prognostic visual acuity was 0.43. However, the one-arm study revealed the inner nuclear layer (INL) was thickened in NMOSD-related-ON eyes compared with HC eyes.

Conclusions: Inclusion of the RNFL and macular GC-IPL is recommended for monitoring disease progression and attention should be paid to changes in the INL.

1. Introduction

Neuromyelitis optica spectrum disorders (NMOSD), a group of neuroinflammatory demyelinating diseases, mainly affect the optic nerve and spinal cord and generally follow a relapsing course.¹ Due to fatal blindness and cumulative disability after NMOSD, effective evaluation of damage has become a major concern.^{2,3} It is possible to quantify the retinal structure in vivo with the application of spectral domain optical coherence tomography (SD-OCT), a non-invasive, repeatable and highly-resolution imaging technique,⁴ which has been widely used to help diagnose ophthalmic and neurodegenerative diseases and which played a significant role in the follow-up of NMOSD. Moreover, it helps to differentiate NMOSD from multiple sclerosis (MS), which reveals that the peripapillary retinal nerve fiber layer (pRNFL) and ganglion cell layer

(GCL) are more severely affected in NMOSD than in MS.⁵ Although a limited number of meta-analysis about NMOSD have been published,⁶ they mainly focused on the retinal nerve fiber layer (RNFL) or GCL. Other layers of the retina, such as the inner plexiform layer (IPL), inner nuclear layer (INL), outer plexiform layer (OPL), and outer nuclear layer (ONL), have not been systematically analyzed, and no systematic review has comprehensively analyzed these layers to date.

In this study, we mainly aimed to systematically review the literature and compare the different retinal layer segmentation damage in NMOSD-related-optic neuritis (ON) with MS, healthy control (HC), and idiopathic optic neuritis (ION), and to further analyze the relationship between retinal structural damage and visual outcome.

* Corresponding author. Fuxing Road No.28, Haidian District, 100853, Beijing, China.)

E-mail address: weishihui706@hotmail.com (S. Wei).<https://doi.org/10.1016/j.aopr.2021.100007>

Received 16 August 2021; Received in revised form 5 September 2021; Accepted 25 September 2021

Available online 5 October 2021

2667-3762/© 2021 The Author(s). Published by Elsevier Inc. on behalf of Zhejiang University Press. This is an open access article under the CC BY-NC-ND license

<http://creativecommons.org/licenses/by-nc-nd/4.0/>.

2. Methods

This study was approved by the Ethics Committee of the Chinese People's Liberation Army General Hospital (Grant No.: S2017-093-01), and it was conducted in accordance with the tenets of the Declaration of Helsinki.

2.1. Search strategy

This meta-analysis was conducted based on the statement of Preferred Reporting Items for Systematic Reviews and Meta-Analyses (PRISMA), and the systematic review and meta-analysis was registered with PROSPERO International Prospective Register of Ongoing Systematic Reviews (Registration number: CRD42020209281). We performed a systematic search for studies in English language from inception to September 1st, 2021. Two reviewers independently searched the following four databases: PubMed, Embase, Cochrane Library, and Web of Science using the strategy of the combination of subject words and free words. For NMOSD, we used "Neuromyelitis Optica", "Aquaporin 4" combined with "Optic Neuritis" as the medical subject heading terms (MeSH terms) for the Pubmed database, whereas "optical coherence tomography device" was used as the stem of the Embase tree. We used "optic neuriti*", "neuropapilliti*", "anterior optic neuriti*", "retrobulbar neuriti*", "posterior optic neuriti*", "acute optic neuritis", "inflammatory optic neuropath*", "neuritis optica", and "optic neuritis" as free words. The detailed search terms and strategies, as well as the included articles, are shown in [Supplement 1](#).

2.2. Study selection

We excluded articles that did not include patients with NMOSD, perform SD-OCT, and separate eyes with ON in patients who had NMOSD (NMOSD+ON eyes) from eyes in patients who had NMOSD without ON (NMOSD-ON eyes), or articles that presented repetitive data already published in the same cohort, or the reported data in a format that could not be translated to mean (SD). To minimize the effect of optic disc swelling, we excluded the articles in which the interval between OCT examination and the last onset was less than 3 months. The article types, including case reports, conference papers, reviews, grey literature, or articles that presented findings at a cellular level or in animals, were also excluded. Articles that did not include a group of control patients were also excluded if they did not include the data on comparison of NMOSD+ON eye with NMOSD-ON eyes, ION eyes, HC eyes, or eyes in patients who had MS with or without a prior history of ON (MS+ON eye or MS-ON eyes). Disagreements were resolved by discussion between the two authors. If the authors did not reach a consensus, a third author (Tan) was invited to resolve the conflicts.

2.3. Data extraction and quality assessment

Two reviews (Fu and Zhou) independently extracted the data. The following data were extracted: the first author, the publication year, type of OCT used, the source of patients, demographic characteristics, including the number of eyes in every subgroup, present ages, percentage of females, disease duration, best-corrected visual acuity (BCVA, all converted to logMAR visual acuity), expanded disability status scale (EDSS), episode of ON, mean thickness of the individual retinal layer in eyes of patients with NMOSD, MS (with and without a history of ON eyes), and ION, and HC participants. Data were reported for the RNFL at the optic disc and macula, but data for other layers were reported only at the macula. The main outcome measure was the thickness (μm) of pRNFL and macular RNFL (mRNFL), a combination of macular ganglion cell layer and inner plexiform layer (GC-IPL), INL, ONL. For the case series, JBI's quality assessment tool, including 10 items, was used. For the case-control study, the Newcastle-Ottawa Scale (NOS) was used for performing evaluation from the following three perspectives: selection,

comparability, and exposure. A study with a NOS score ≥ 6 or JBI score ≥ 6 was considered to have high quality.

2.4. Statistical analysis

Meta-analysis was conducted using Stata 14, RevMan 5.4, and GraphPad Prism 8.0.2 (GraphPad Software, USA). All of the outcomes were continuous variables. One-arm meta-analysis was performed to determine the thickness of the retina layer in each subgroup. To compare the difference between each group in pairs, we conducted a meta-analysis of dual-arm studies. Both meta-analysis used I^2 to evaluate the heterogeneity among studies. When $I^2 < 50\%$, the heterogeneity was regarded as acceptable and a fixed-effect model was used, however, the source of heterogeneity was analyzed and a random-effects model was used to minimize the impact of heterogeneity. Publication bias was shown by funnel plot if the number of studies was greater than 10. For the correlation analysis between the thickness of the retinal layer and prognostic BCVA (logMAR), we firstly transformed the extracted data as follows below, and then meta-analysis was carried out with RevMan 5.4 software. The following conversion formula was used:

- ① fisher's Z = $0.5 \times \ln \frac{1+r}{1-r}$
- ② $V_Z = \frac{1}{n-3}$
- ③ $S_E = \sqrt{V_Z}$
- ④ Summary r = $\frac{e^{2Z}-1}{e^{2Z}+1}$ (Z is the value of summary fisher's Z)

The r is the correlation between the thickness of the retinal layer and prognostic BCVA. According to the above formula, we calculated the Fisher's Z and S_E , then we input them to the RevMan 5.4 software. Using the inverse variance method, we acquired the summary of Fisher's Z.⁷ Finally, we translated the Fisher's Z to summary r based on formula ④. The summary r was the final coefficient.

3. Results

3.1. Study characteristics and quality assessment

Nine hundred and fifty-three records were retrieved from 4 electronic databases. A total of 42 studies were included in our systematic review for qualitative synthesis with the year of publication from 2009 to September 1st, 2021.⁸⁻⁴⁹ All studies included in our review were considered to be of high quality, and the details of quality assessment are provided in [Table S1](#) and [Table S2](#). The reported mean or median duration of the disease was more than 6 months. According to the recording, 38 of these studies including 3273 patients (1344 patients with NMOSD, 850 patients with MS, 938 HCs, and 141 patients with ION). In total, there were 2470 females and 689 males according to the original literature. With respect to the eyes, 6288 eyes were included in the study (1704 NMOSD+ON eyes, 708 NMOSD-ON eyes, 1914 HC eyes, 851 MS+ON eyes, 956 MS-ON eyes, and 155 ION eyes). Nearly all of the patients were adults, with the mean or median age range from 25.02 to 50.2 years. [Fig. 1](#) summarizes the flow diagram of the literature screening. A total of 4 devices of SD-OCT were used in the studies (Topcon, Cirrus, Heidelberg, and Optovue). The demographic characteristics of the included studies are shown in [Table 1](#). The patients were recruited from 16 countries (China, Italy, USA, Australia, Brazil, Turkey, Germany, Thailand, Korea, Japan, Spain, Canada, Poland, Iraq, Oxford and Berlin).

3.2. Qualitative analysis

[Table 2](#) summarizes the comparison for pRNFL, mRNFL, GC-IPL, INL, ONL between groups.

A significant reduction in the pRNFL occurred in NMOSD eyes with or without ON compared with HC eyes, and the attenuation in NMOSD+ON

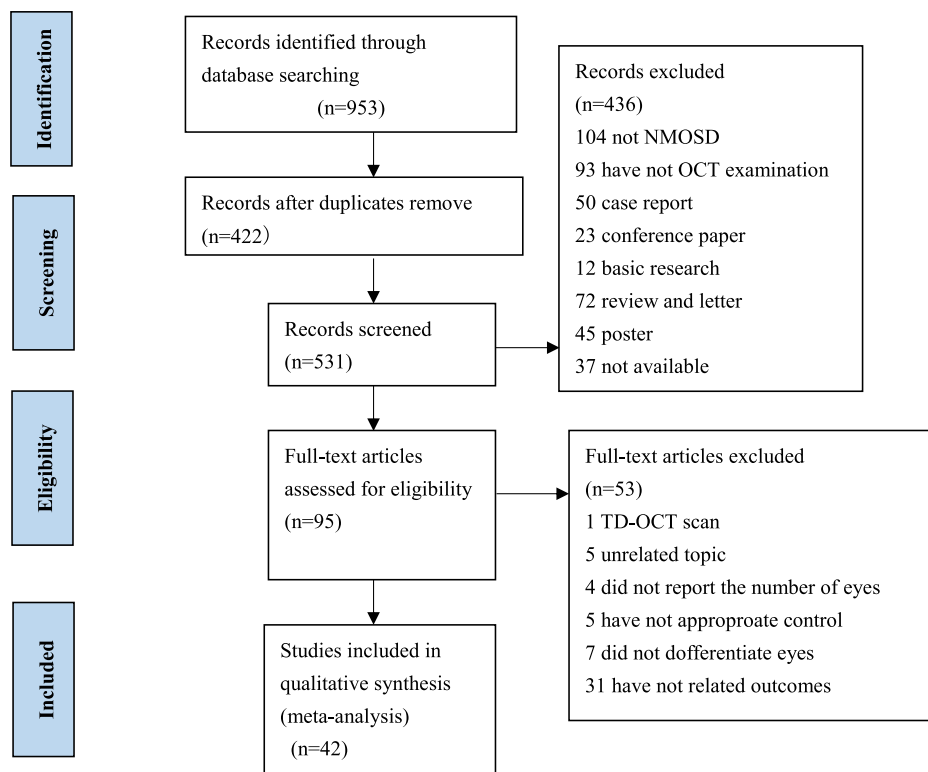


Fig. 1. The flow diagram of the screening of the literature.

eyes was greater [-2.77 (-3.13,-2.40), CI < 0.001; -0.63 (-1.00,-0.25), $P < 0.001$] (Fig. 2, Fig. S1). On comparing the eyes of patients with NMOSD, the same result was obtained [-1.70 (-1.98,-1.40), $P < 0.001$] (Fig. S2). Also, atrophy of the pRNFL in NMOSD+ON eyes was greater than that in MS+ON eyes [-1.25 (-1.62,-0.87), $P < 0.001$] (Fig. S3). However, on comparing NMOSD-ON eyes with MS-ON eyes, we did not obtain any meaningful results [0.11 (-0.06,0.28), $P = 0.09$] (Fig. S4). Due to limited data, we only compared the NMOSD+ON eyes with ION eyes, and the results revealed that NMOSD eyes had thinner pRNFL than ION eyes [-1.90 (-3.25,-0.56), $P < 0.001$] (Fig. S5). Specifically, that one-arm meta-analysis showed that thickness of the pRNFL in ION eyes was merely 69.31 μm , in contrast, the thickness of the pRNFL was 58.83 μm in NMOSD+ON eyes, 77.92 μm in MS+ON eyes, 102.26 μm in HC eyes (Figs. S6–S10), and the results are shown in Table 3 and Fig. 4. The heterogeneity among the studies was high, therefore, a random-effects model was considered except for the NMOSD-ON versus MS-ON comparison. Publication bias was found in each comparison (Figs. S46–S55).

The meta-analysis for mRNFL indicated atrophy in NMOSD+ON eyes compared with NMOSD-ON or HC eyes, though we only included 2 or 3 studies respectively [-1.03 (-1.81,-0.26), $P = 0.046$; -1.72 (-2.41,-1.03), $P < 0.001$] (Figs. S11–S12). Though we did not find any statistical differences between NMOSD+ON eyes and MS+ON eyes [-0.36 (-1.06, 0.35), $P = 0.105$] (Fig. S13), the one-arm analysis showed that the thickness of the mRNFL was relatively lesser in NMOSD+ON eyes than in MS+ON eyes (23.29 μm and 28.41 μm , respectively) (Figs. S15 and S18). Similarly, in NMOSD-ON eyes, thickness of the mRNFL was slightly less when compared with that in HC eyes (29.72 μm and 32.76 μm , separately) (Figs. S16 and S17) while no statistical significance was found between them [-0.72 (-1.04,-0.39), $P = 0.239$] (Fig. S14).

On comparing the eyes of patients with NMOSD, as expected, a thinned GC-IPL was observed in NMOSD+ON eyes compared with NMOSD-ON eyes [-1.45 (-1.89,-1.01), $P < 0.001$] (Fig. S20), and atrophy of the GC-IPL in NMOSD+ON eyes was evident compared with that in HC eyes [-2.65 (-3.29,-2.00), $P < 0.001$] (Fig. S21). The mean difference between the NMOSD-ON eyes and HC eyes indicated thinning of the GC-

IPL in NMOSD-ON eyes [-0.68 (-1.00,-0.37), $P = 0.012$] (Fig. S22). The meta-analysis for the GC-IPL showed that no change in thickness occurred in MS+ON eyes versus NMOSD+ON eyes or MS-ON eyes versus NMOSD-ON eyes, respectively [-0.80 (-1.02,-0.59), $P = 0.127$; 0.06 (-0.28,0.40), $P = 0.289$] (Figs. S23–24). Actually, the thickness of the GC-IPL in NMOSD+ON, NMOSD-ON, HC, MS+ON, MS-ON subgroup was 60.14 μm , 82.91 μm , 82.53 μm , 61.50 μm , and 71.09 μm , respectively (Table 3 and Fig. 4) (Figs. S25–29).

As depicted in Figs. S30–36 for the INL, there was a lack of an adequate database to compare NMOSD-ON eyes with other eyes because only one study reported thickness of the INL in NMOSD-ON eyes. One-arm analysis showed that when NMOSD+ON eyes were compared with HC or MS+ON eyes, thickening of the INL was prominent in NMOSD+ON eyes (40.30 μm > 37.76 μm > 36.68 μm) (Figs. S32, S34, S35), although we did not derive a statistically significant conclusion (95% confidence intervals contain 0) (Figs. S30 and S31).

The meta-analysis for thickness of the ONL demonstrated that no statistical significance existed in each group based on the fact that the 95% confidence interval went through 0 (Figs. S37–S40). Nevertheless, one-arm pooled results showed that the specific thickness of the ONL in each subgroup was 79.33 μm in the NMOSD+ON group, 92.95 μm in the NMOSD-ON group, 68.75 μm in the MS+ON group, 64 μm in the MS-ON group, 88.47 μm in the HC group, thickening was noted in NMOSD eyes than in MS eyes (Figs. S41–S45).

Publication bias was not found for mRNFL, GC-IPL, INL, ONL because the number of studies with available data was not more than ten. Overall, for comparisons between groups, the largest effect sizes were seen for the pRNFL and GC-IPL, where the effect sizes were small for the mRNFL, INL, and ONL.

We intended to conduct a correlation analysis between BCVA and different retinal layer segmentation, but only three studies reported the correlations between BCVA and pRNFL and the meta-analysis revealed the correlation coefficient was 0.43 (Fig. 3), which indicated that prognostic BCVA had a low correlation with pRNFL.

Table 1
Demographic characteristics of the included studies.

Study	OCT device	Country	Group	eyes	age (year, mean ± SD or range)	gender (F/M)	VA (logMAR)	episode of ON	EDSS
Zhang 2020	Zeiss	China	NMO+ON	113	37 (29.5–48)	110/14	0.24 ± 0.43	NA	NA
			NMO-ON	95					
			HC	90					
Peng 2020	Heidelberg	China	NMOSD+ON	62	38 (27–50)	35/7	1.33 ± 1.23	NA	NA
			HC	80					
			ION	40					
Kwamong 2020	Optovue	China	NMOSD+ON	19	48.10 ± 11.79	NA	0.41 ± 0.49	1.61 ± 1.95	NA
			NMOSD-ON	9					
			HC	30					
Chen 2020	Optovue	China	NMOSD+ON	21	50.2 ± 12.5	27/0	0.31 ± 0.43	NA	NA
			NMOSD-ON	26					
			HC	62					
Vabanesi 2019	Heidelberg	Italy	NMOSD+ON	56	44.9 ± 12.7	43/7	0.46	NA	NA
			NMOSD-ON	44					
			MS+ON	55					
Sotirchos 2019	Zeiss	USA	AQP4+ON	48	43.7 ± 12.7	43/5	NA	1 (1–5)	NA
			MS+ON	40					
			HC	31					
Shen 2019	Heidelberg	Australia	NMOSD+ON	15	48.2 ± 16.1	13/6	0.70 ± 1.03	NA	NA
			NMOSD-ON	4					
			MS+ON	67					
Pisa 2019	Heidelberg	Italy	NMOSD+ON	43	46.2 ± 13.3	NA	NA	NA	3.31 ± 2
			NMOSD-ON	19					
			MS+ON	46					
Huang 2019	Optovue	China	NMOSD+ON	52	40.8 ± 13.0	52/3	NA	NA	2 (1–7.5)
			NMOSD-ON	56					
			HC	66					
Filgueiras 2019	Heidelberg	Brazil	NMOSD+ON	23	35.03 ± 11.14	25/5	NA	NA	NA
			NMOSD-ON	27					
			MS+ON	22					
Çolpak 2019	Heidelberg	Turkey	NMOSD+ON	57	45.37 ± 10.58	20/9	NA	NA	NA
			NMO+ON	15					
			NMO-ON	11					
Zhao 1 2018	Heidelberg	China	NMOSD+ON	59	35 (20.75–47)	46/6	2.17 ± 1.38	NA	NA
			HC	60					
			ION	93					
Tian 2018	Optovue	China	NMO+ON	48	40.8 ± 14.8	20/4	0.5 (0.2–2)	NA	3.75 (1–8.5)
			NMO-ON	24					
			HC	48					
Oertel 2018	Heidelberg	German	NMOSD+ON	34	47.3 ± 14.4	43/8	NA	NA	3 (0–6)
			NMOSD-ON	60					
			HC	56					
Mekhasingharak 2018	Zeiss	Thailand	AQP4+ON	43	34.5 ± 13.8	24/1	0.76 ± 0.88	NA	NA
			MS+ON	17					
			HC	30					
Kim 2018	Zeiss	Korea	NMOSD+ON	101	39.4 ± 12.0	63/10	1.00 [-0.1–3.0]	1 (0–12)	3.9 ± 1.9
			NMOSD-ON	45					
			HC	30					
Hu 2018	Zeiss	China	NMO+ON	30	26 ± 10.21	18/12	(0.3–1.3)	NA	NA
			NMO-ON	10					
			HC	30					
Peng 2017	Heidelberg	China	AQP4+ON	54	38.41 ± 13.00	eye 45/9	1.22 ± 1.19 (0–3.7)	1.70 ± 0.86 (1–4)	NA
			NMO+ON	42					
			HC	94					
Matsumoto 2017	Optovue	Japan	AQP4+ON	20	43 (10–64)	10/2	0.05 (-0.18-3)	NA	NA
			MS+ON	40					
			HC	31					

(continued on next page)

Table 1 (continued)

study	OCT device	Country	Group	eyes	age (year, mean ± SD or range)	gender (F/M)	VA (logMAR)	episode of ON	EDSS
Peng 2016	Heidelberg	China	AQP4+ON	66	38.4 ± 13.6	36/9	1.31 ± 1.25	NA	NA
			HC	88	40.1 ± 14.3	31/18	NA	NA	NA
Pache 2016	Heidelberg	Europe	AQP4+ON	21	34.7 ± 14.8	16/0	0.72 ± 1.09	2 (1-4)	4 (1-6.5)
			HC	28	NA	NA	NA	NA	NA
Martinez-Lapiscina 2016	Heidelberg	Spain	AQP4+NMOSD+ON	9	NA	6/3	NA	2 (1-3.5)	NA
			MOG+NMOSD+ON	6	NA	3/3	NA	2 (1-2)	NA
			MS+ON	15	NA	9/6	NA	NA	NA
Manogaran 2016	Heidelberg	Canada	NMO+ON	13	47.9 ± 13	6/2	0.15	NA	2.5 (2-6)
			NMO-ON	6	39 ± 3	1/1	0	NA	2.5 (2.5-2.5)
			MS+ON	21	38.3 ± 9.7	9/7	0.1	NA	2 (0-4)
			MS-ON	63	40.3 ± 9.6	16/10	0.1	NA	1.75 (0-4)
Jeong 2016	Zeiss	Korea	HC	22	31.2 ± 9.6	9/3	NA	NA	NA
			NMOSD+ON	99	39.7 ± 11.8	62/10	1 (-0.1-3)	1 (0-12)	3.5 (1-8.5)
			NMOSD-ON	45	NA	NA	0.1 (-0.1-3)	NA	NA
			HC	68	39.4 ± 11.2	10/24	0.1 (-0.1-1.6)	NA	NA
Cheng 2016	Heidelberg	China	NMO+ON	41	42.41 ± 9.98	20/6	0.15 (0-2.0)	NA	NA
			HC	52	42.06 ± 10.54	20/6	0 (0, 0.10)	NA	NA
Park 2014	Heidelberg	Korea	NMO+ON	19	43.67 ± 2.69	13/7	1.00 ± 0.32	NA	NA
			MS+ON	15	32.00 ± 3.36	11/5	0.32 ± 0.22	NA	NA
			HC	24	41.42 ± 12.41	16/8	0 ± 0	NA	NA
			ION	22	48.05 ± 2.60	10/10	0.40 ± 0.15	NA	NA
study	OCT device	Country	group	Eyes	age (year, mean ± SD or range)	gender (F/M)	VA (logMAR)	episode of ON	EDSS
Sotirchos 2013	Zeiss	USA	NMO/AQP4+ON	45	43.1 ± 13.4	26/5	NA	1.57 ± 1.41 (1-10)	NA
			NMOSD-ON	28	NA	NA	NA	NA	NA
			HC	78	43.5 ± 13.5	34/5	NA	NA	NA
Schneider 2013	Heidelberg	German	NMOSD+ON	20	40.8 ± 12.3	16/1	NA	NA	NA
			MS+ON	20	41.2 ± 12.7	16/1	NA	NA	NA
Lange 2013	Heidelberg	Canada	HC	34	41.4 ± 12.4	16/1	NA	NA	NA
			NMO+ON	32	49.60 ± 12.94	22/3	NA	NA	2.5 (0-8)
			NMO-ON	18	NA	NA	NA	NA	NA
			MS+ON	13	43.5 ± 9.1	23/2	NA	NA	2.5 (1-6.5)
Hokazono 2013	Topcon	Brazil	MS-ON	37	NA	NA	NA	NA	NA
			HC	100	49.2 ± 10.2	27/23	NA	NA	NA
			NMO+ON	30	39.6 ± 13.1	18/2	0.1	NA	NA
			MS+ON	29	36.75 ± 11.45	24/4	0	NA	NA
Syc 2012	Zeiss	USA	MS-ON	22	NA	NA	0	NA	NA
			HC	30	36 ± 12.5	13/13	0	NA	NA
			NMO+ON	17	48.3 ± 9.9	19/3	NA	NA	NA
			NMO-ON	23	NA	NA	NA	NA	NA
			MS+ON	73	41.7 ± 10.8	70/28	NA	NA	NA
			MS-ON	123	NA	NA	NA	NA	NA
			HC	144	42.39 ± 8.14	16/6	NA	NA	NA
study	OCT device	Country	group	Eyes	age (year, mean ± SD or range)	gender (F/M)	VA (logMAR)	episode of ON	EDSS
Monteiro 2012	Topcon	Brazil	NMO+ON	51	39.9 ± 11.6	30/3	0.1	NA	NA
			MS+ON	45	35.6 ± 9.4	50/10	0	NA	NA
			MS-ON	74	NA	NA	0	NA	NA
			HC	82	36.6 ± 12.3	35/6	0	NA	NA
Nakamura 2010	Zeiss	Japan	NMO+ON	27	36.1 ± 12.3	18/0	1.74	NA	NA
			NMO-ON	8	NA	NA	-0.1	NA	NA
			MS+ON	19	30.2 ± 10.4	12/2	-0.2	NA	NA
			MS-ON	9	NA	NA	-0.1	NA	NA
Ratchford 2009	Zeiss	USA	NMOSD+ON	22	41 ± 13	NA	NA	NA	NA
			NMOSD-ON	8	NA	NA	NA	NA	NA
			MS+ON	157	39 ± 10	NA	NA	NA	NA
			MS-ON	338	NA	NA	NA	NA	NA
Naismith 2009	Stratus OCT	USA	HC	77	38 ± 12	NA	NA	NA	NA
			NMO+ON	30	42.9 (24-64)	77/23	0.1	1.61 (1, 0-6)	4 (4.5,0-8.5)
Green 2009	Stratus OCT	USA	MS+ON	65	42.3 (22-65)	83/17	0	0.97 (1, 0-5)	2 (2.7,0-7)
			NMO+ON	27	41 ± 11.7	14/2	NA	NA	NA
Zeng 2021	Optovue	China	MS+ON	24	41 ± 11.7	16/4	NA	NA	NA
			NMOSD+ON	55	44.18 ± 16.06	49/1	0.76 ± 0.04	1.04 ± 0.32	4.38 ± 3.17
			NMOSD-ON	45	NA	49/1	0.18 ± 0.02	NA	NA
			HC	20	44.43 ± 12.90	9/1	0.08 ± 0.12	NA	NA
Study	OCT device	Country	Group	Eyes	age (year, mean ± SD or range)	gender (F/M)	VA (logMAR)	episode of ON	EDSS
Rogaczewska 2021	Optovue	Poland	NMOSD+ON	9	42.08 ± 10.23	11/2	0 (0-2.3)	NA	NA
			NMOSD-ON	11	NA	11/2	0 (0-2.3)	NA	NA
			MS+ON	30	35.15 ± 7.47	32/8	0 (0-0.2)	NA	NA
			MS-ON	45	NA	32/8	0 (0-0.2)	NA	NA

(continued on next page)

Table 1 (continued)

Study	OCT device	Country	Group	Eyes	age (year, mean ± SD or range)	gender (F/M)	VA (logMAR)	episode of ON	EDSS
Roca-Fernández 2021	Heidelberg	Oxford and Berlin	HC	40	37.90 ± 11.47	17/3	0 (0-0)	NA	NA
			NMOSD+ON	15	37.77 ± 19.72	10/2	NA	NA	NA
			NMOSD-ON	34	45.64 ± 10.97	20/1	NA	NA	NA
AbdulRasool 2020	Optovue	Iraq	HC	76	41.61 ± 16.27	27/11	NA	NA	NA
			NMOSD+ON	43	(18-50)	NA	NA	NA	NA
			NMOSD-ON	22	(18-50)	NA	NA	NA	NA
			MS+ON	50	(18-50)	NA	NA	NA	NA
Yu1 2021	Optovue	China	MS-ON	31	(18-50)	NA	NA	NA	NA
			AQP4+ON	43	40 ± 10	23/1	0.36 ± 0.52	2.13 ± 0.77	NA
			HC	50	39 ± 8	20/5	0.00 ± 0.04	NA	NA
Yu2 2021	Optovue	China	NMOSD+ON	66	44 ± 12	46/2	0.48 ± 0.84	NA	NA
			NMOSD-ON	30		46/2	0 ± 0	NA	NA
			HC	40	45 ± 10	19/1	0 ± 0	NA	NA

4. Discussion

Recent studies have analyzed the anterior visual pathway using full-field visual evoked potentials (ffVEP) and SD-OCT, as well as MRI scans of the brain and spinal cord, and they suggested subclinical disease activity in NMOSD without clinical ON.⁵⁰⁻⁵² This study provided relatively detailed information about retinal structure in NMOSD with or without ON and compared it with other subgroups. Although both NMOSD and MS are neurodegenerative diseases, the difference in pathogenesis leads to the difference in clinical manifestations. OCT, a useful instrument in the follow-up of NMOSD, is an accurate means to monitor the loss of retinal layer segmentation damage.⁵

This meta-analysis, including 42 observational studies, reveals that NMOSD+ON eyes had a loss of the GC-IPL and a thinner pRNFL compared with HC eyes, which indicated that NMOSD patients had atrophy of retinal ganglion cells body and their axons. Furthermore, it was evident that the decrease in the thickness of the pRNFL and GC-IPL was more obvious in NMOSD+ON eyes owing to inflammation and necrosis, with more prominent neuronal and axonal damage than NMOSD-ON eyes. Correlation analysis suggested that pRNFL thinning was associated with poor prognostic visual acuity in NMOSD+ON eyes ($r = 0.43$), which implied that we can evaluate the prognostic visual acuity by measuring thickness of the pRNFL.

When focusing on mRNFL, the thickness in NMOSD+ON eyes was lesser compared with that in NMOSD-ON or HC eyes. However, in NMOSD-ON eyes, the mRNFL had no significant outcome compared with the HC eye. It should be remembered that only 2 studies were included for mRNFL. Conversely, the one-arm analysis revealed that a thinner mRNFL existed in NMOSD-ON eyes than HC eyes ($29.72 \mu\text{m} < 32.76 \mu\text{m}$). Currently, it is believed that the pathogenesis of NMOSD is mainly mediated by AQP4 antibody,⁵³ and we speculated that "Müller cells", running vertically from the inner limiting membrane to the outer limiting membrane, expressing AQP4 in the fovea and peripheral retinas, are vital to the functions and vitality of RGCs, combined with the assumption that retinal astrocytes might be the target of AQP4-Ab, which may account for a subclinical loss of RNFL and GC-IPL even when there is no history of ON. These findings above imply that NMOSD is a primary retinopathy that is highly probable to a lack of energy due to targeted attacks and decreased retinal perfusion.¹⁶

When compared with MS+ON or ION eyes, atrophy of the pRNFL occurs in NMOSD+ON eyes. However, dual-arm studies displayed that no thinning was found in the mRNFL and GC-IPL. At the same time, we found that the P-value of the latter two fluctuated around 0.1. Therefore, it might be attributed to an inadequate number of samples (all under five, less than ten). For NMOSD-ON eyes, when compared with MS-ON eyes, significant results could not be acquired in terms of the pRNFL and GC-IPL. In other words, there was no evident difference in any retinal layer between NMOSD eyes and MS eyes without ON.

On the contrary, the INL of NMOSD+ON eyes was slightly thickened when compared with that of HC eyes, which is consistent with the result

of one-arm study ($39.47 \mu\text{m} > 37.63 \mu\text{m}$). Therefore, we hypothesized that progressive inflammation of the retina may occur in the chronic phase of NMOSD+ON. Similarly, we did not find any remarkable result in thickness of the INL when comparing NMOSD+ON eyes with MS+ON eyes, and the specific thickness of the INL in each group (NMOSD+ON, NMOSD-ON, MS+ON, MS-ON, and HC) was $40.30 \mu\text{m}$, $35.40 \mu\text{m}$, $36.68 \mu\text{m}$, $32.69 \mu\text{m}$, $37.76 \mu\text{m}$, respectively. We can state that NMOSD+ON eyes have a slightly thicker INL when compared with HC eyes. In consequence, we modestly speculated that inflammation is present in NMOSD+ON eyes. When we concentrated on NMOSD or MS without ON eyes, we could not achieve any valuable outcome due to limited studies. Simultaneously, we could not obtain more information about the thickness variation of ONL due to fewer studies. As already known, our human visual pathway consists of three levels of neurons, the first bipolar neuron in the retina, the second retinal ganglion cells, and the third body of neurons located in the lateral geniculate nucleus; any irreversible axonal damage in this pathway will lead to retrograde trans-synaptic axonal degeneration, which will cause atrophy of the inner retinal layers. Trans-synaptic degeneration may stop at the INL, which contains the first bipolar neuron and probably acts as a physiological barrier to retrograde trans-synaptic degeneration. This feature renders the INL an attractive layer for the investigation of inflammation.⁵⁴ Swelling of the INL after ON suggests that a specific type of inflammation may exist in NMOSD, which is consistent with the findings that approximately 20% of NMOSD patients have microcystic alterations of the INL.⁵⁵

These new quantitative layer segmentation data extended the earlier pRNFL data by showing that the loss of cell body and axon of RGCs was severe after ON associated with NMOSD and a specific type of inflammation may exist in INL during the chronic phase, but we did not have enough evidence to compare it with corresponding MS eyes. The result was consistent with the most important recent publications on OCT in NMOSD.^{31,34,35,38-42,56-61} To sum up, it is reasonable to postulate that subclinical loss of retinal ganglion cells existed in NMOSD patients, and NMOSD+ON eyes may have progressive chronic inflammation.

There are some advantages of our meta-analysis; this is the first largest meta-analysis of different retinal layer segmentation in NMOSD based on SD-OCT. This outcome emphasizes the underlying neurodegeneration and inflammation of the INL in NMOSD, especially after ON. We further uncovered the potential correlation between the prognostic BCVA and retinal structure. However, this study has several limitations. First, although this meta-analysis comprehensively provided a valuable summary of the available data on thickness of all retinal layers from pRNFL to ONL in NMOSD, it was to original researches, only observational studies, either case-control studies or case-series studies, were included, which may cause selection bias. Second, because of the restricted study group, especially when compared with MS in mRNFL, INL, and ONL, we could not derive certain conclusions in some points; hence, a larger-scale, multicentre, international collaborative prospective study is required to enhance the statistical power. Further, in some

Table 2

The results of the dual-arm meta-analysis for retinal layer segmentation in each subgroup.

	studies (N.)	Random/fixed effects, (I ²)	SMD, 95%CI	P-value
pRNFL (µm)				
NMOSD+ON vs. NMOSD-ON	28	Random (84.9%)	-1.70 (-1.98,-1.40)	<0.001
NMOSD+ON vs. HC	32	Random (92.2%)	-2.77 (-3.13,-2.40)	<0.001
NMOSD+ON vs. MS+ON	21	Random (88.6%)	-1.25 (-1.62,-0.87)	<0.001
NMOSD-ON vs. HC	22	Random (92.2%)	-0.63 (-1.00,-0.25)	<0.001
NMOSD-ON vs. MS-ON	11	fixed (37.6%)	0.11 (-0.06,0.28)	0.09
NMOSD+ON vs. ION	3	Random (95.2%)	-1.90 (-3.25,-0.56)	<0.001
mRNFL (µm)				
NMOSD+ON vs. NMOSD-ON	2	Random (74.8%)	-1.03 (-1.81,-0.26)	0.046
NMOSD+ON vs. HC	3	Random (79.6%)	-1.72 (-2.41,-1.03)	<0.001
NMOSD+ON vs. MS+ON	2	Random (62.0%)	-0.36 (-1.06,0.35)	0.105
NMOSD-ON vs. HC	2	Fixed (27.8%)	-0.72 (-1.04,-0.39)	0.239
INL (µm)				
NMOSD+ON vs. NMOSD-ON	9	Random (79.0%)	-1.45 (-1.89,-1.01)	<0.001
NMOSD+ON vs. HC	10	Random (92.9%)	-2.65 (-3.29,-2.00)	<0.001
NMOSD+ON vs. MS+ON	5	fixed (44.2%)	-0.80 (-1.02,-0.59)	0.127
NMOSD-ON vs. HC	7	Random (63.4%)	-0.68 (-1.00,-0.37)	0.012
NMOSD-ON vs. MS-ON	3	fixed (19.4%)	0.06 (-0.28,0.40)	0.289
ONL (µm)				
NMOSD+ON vs. NMOSD-ON	2	Random (82.1%)	0.25 (-0.63,1.12)	0.018
NMOSD+ON vs. HC	3	Random (55.9%)	-0.22 (-0.56,0.12)	0.103
NMOSD+ON vs. MS+ON	3	Random (81.5%)	-0.13 (-0.88,0.62)	0.005
NMOSD-ON vs. HC	2	Random (83.5%)	-0.28 (-1.06,0.51)	0.014
NMOSD-ON vs. MS-ON	NA			

pRNFL peripapillary retinal nerve fiber layer, mRNFL macular retinal nerve fiber layer, GC-IPL ganglion cell and inner plexiform layer, INL inner nuclear layer, ONL outer nuclear layer, NMOSD+ON neuromyelitis optica spectrum disorder-related optic neuritis, MS+ON multiple sclerosis-related optic neuritis, NMOSD-ON neuromyelitis optica spectrum disorder without optic neuritis, MS-ON multiple sclerosis without optic neuritis, ION idiopathic optic neuritis, HC healthy control.

included studies, the time interval between SD-OCT examination and last ON attack was merely more than 3 months, the relatively inadequate follow-up time may have affected the results. Therefore, further long-term follow-up studies are necessary to provide more evidence and to show the extent of usefulness of OCT for the study of NMOSD. Finally, limited to the original researches, we only performed structural and

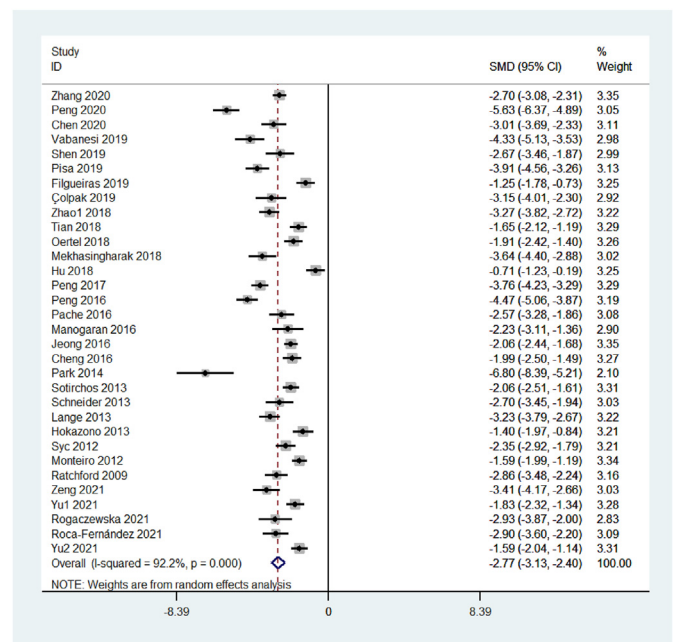


Fig. 2. Forest plot showing the dual-arm meta-analysis result of pRNFL thickness between NMOSD+ON and HC eyes. SMD standard mean difference, CI confidence interval.

Table 3

The thickness of different retinal layer segmentation in different subgroup eyes.

Subgroup	NMOSD+ON	NMOSD-ON	MS+ON	MS-ON	HC	ION
N	42	28	21	14	32	3
pRNFL (µm)	58.83	99.81	77.92	94.52	102.26	69.31
N	12	9	5	3	10	
GC-IPL (µm)	60.14	82.91	61.5	71.09	82.53	NA
N	3	2	2	1	3	
mRNFL (µm)	23.29	29.72	28.41	29.83	32.76	NA
N	5	1	5	2	4	
INL (µm)	40.3	35.4	36.68	32.69	37.76	NA
N	4	2	3	1	3	
ONL (µm)	79.33	92.95	68.75	64	88.47	NA

pRNFL peripapillary retinal nerve fiber layer, mRNFL macular retinal nerve fiber layer, GC-IPL ganglion cell and inner plexiform layer, INL inner nuclear layer, ONL outer nuclear layer, NMOSD+ON neuromyelitis optica spectrum disorder-related optic neuritis, MS+ON multiple sclerosis-related optic neuritis, NMOSD-ON neuromyelitis optica spectrum disorder without optic neuritis, MS-ON multiple sclerosis without optic neuritis, ION idiopathic optic neuritis, HC healthy control, vs versus.

functional correlation analysis of the pRNFL and it was difficult to further analyze the consistent changes in the imaging structure and tissue structure due to the difficulty in obtaining human retina.

5. Conclusions

This systematic review and meta-analysis indicated that subclinical loss of retinal RNFL and GC-IPL exists in NMOSD eyes even when there is no history of ON. Besides, the damage to the body and axons of RGCs is more severe in NMOSD eye with an episode of ON. Progressive inflammation of the INL may occur in NMOSD eyes with ON. Inclusion of the RNFL and macular GC-IPL is recommended for monitoring disease progression and attention should be paid to the changes in the INL.

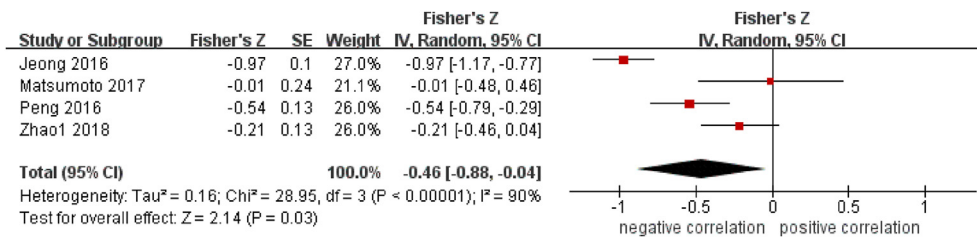


Fig. 3. The correction between BCVA (LogMAR) and pRNFL in NMOSD+ON eyes. BCVA best-corrected visual acuity, pRNFL peripapillary retinal nerve fiber layer, NMOSD+ON neuromyelitis optica spectrum disorder-related optic neuritis, CI confidence interval.

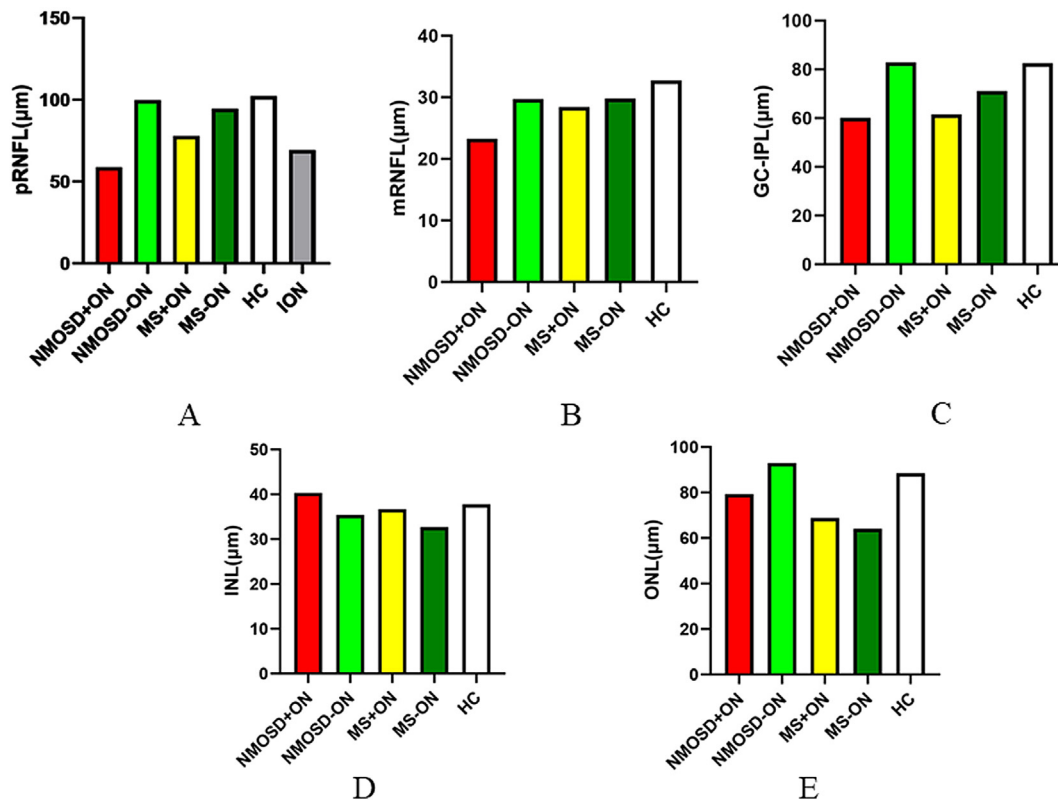


Fig. 4. Comparisons of the thickness of different retinal layer segmentation in different subgroup eyes. (A) Comparisons of the thickness of pRNFL in NMOSD+ON, NMOSD-ON, MS+ON, MS-ON, HC, and ION eyes. (B) Comparisons of the thickness of mRNFL in NMOSD+ON, NMOSD-ON, MS+ON, MS-ON, and HC eyes. (C) Comparisons of the thickness of GC-IPL in NMOSD+ON, NMOSD-ON, MS+ON, MS-ON, and HC eyes. (D) Comparisons of the thickness of INL in NMOSD+ON, NMOSD-ON, MS+ON, MS-ON, and HC eyes. (E) Comparisons of the thickness of ONL in NMOSD+ON, NMOSD-ON, MS+ON, MS-ON, and HC eyes. NMOSD+ON neuromyelitis optica spectrum disorder-related optic neuritis, NMOSD-ON neuromyelitis optica spectrum disorder without optic neuritis, MS+ON multiple sclerosis-related optic neuritis, MS-ON multiple sclerosis without optic neuritis, HC healthy controls, ION idiopathic optic neuritis, pRNFL peripapillary retinal nerve fiber layer, mRNFL macular retinal nerve fiber layer, GC-IPL ganglion cell and inner plexiform layer, INL inner nuclear layer, ONL outer nuclear layer.

Study Approval

Not applicable.

Author Contributions

Concept and design: JX F, SH W; Acquisition, analysis, and interpretation of data: JX F and HF Z; Drafting of the manuscript: JX F; Revision of the manuscript: JX F, SY T, and CX P; Statistical analysis: JX F. All authors had full access to all the data in the study and were responsible for the integrity and accuracy of data.

Acknowledgements

Thanks to all the peer reviewers for their opinions and suggestions.

Funding

This work was supported by China-USA intergovernmental Cooperation program (2018YFE0113900).

Conflict of Interest

The authors declare that they have no known competing financial interests or personal relationships that could have appeared to influence the work reported in this paper.

Abbreviations

- NMOSD neuromyelitis optica spectrum disorders
- SD-OCT spectral-domain optical coherence tomography
- MS multiple sclerosis

HC	healthy controls
ON	optic neuritis
ION	idiopathic optic neuritis
RNFL	retinal nerve fiber layer
pRNFL	peripapillary retinal nerve fiber layer
mRNFL	macular retinal nerve fiber layer
GCL	ganglion cell layer
INL	inner nuclear layer
IPL	inner plexiform layer
GC-IPL	ganglion cell and inner plexiform layer
OPL	outer plexiform layer
ONL	outer nuclear layer
NMOSD+ON	neuromyelitis optica spectrum disorder-related optic neuritis
NMOSD-ON	neuromyelitis optica spectrum disorder without optic neuritis
MS+ON	multiple sclerosis-related optic neuritis
MS-ON	multiple sclerosis without optic neuritis
ffVEP	full-field visual evoked potentials
BCVA	best-corrected visual acuity
EDSS	expanded disability status scale
PRISMA	Preferred Reporting Items for Systematic Reviews and Meta-Analyses
MeSH terms	medical subject heading terms
NOS	Newcastle-Ottawa Scale

Appendix A. Supplementary data

Supplementary data to this article can be found online at <https://doi.org/10.1016/j.aopr.2021.100007>.

References

- Wingerchuk DM, Banwell B, Bennett JL, et al. International consensus diagnostic criteria for neuromyelitis optica spectrum disorders. *Neurology*. 2015;85(2):177–189. <https://doi.org/10.1212/WNL.0000000000001729>.
- Bruscolini A, Sacchetti M, La Cava M, et al. Diagnosis and management of neuromyelitis optica spectrum disorders - an update. *Autoimmun Rev*. 2018;17(3):195–200. <https://doi.org/10.1016/j.autrev.2018.01.001>.
- Borisov N, Mori M, Kuwabara S, Scheel M, Paul F. Diagnosis and treatment of NMO spectrum disorder and MOG-encephalomyelitis. *Front Neurol*. 2018;9:888. <https://doi.org/10.3389/fneur.2018.00888>.
- Simao LM. The contribution of optical coherence tomography in neurodegenerative diseases. *Curr Opin Ophthalmol*. 2013;24(6):521–527. <https://doi.org/10.1097/ICU.0000000000000000>.
- Mateo J, Esteban O, Martínez M, Grzybowski A, Ascaso FJ. The contribution of optical coherence tomography in neuromyelitis optica spectrum disorders. *Front Neurol*. 2017;8:493. <https://doi.org/10.3389/fneur.2017.00493>.
- Peng A, Qiu X, Zhang L, et al. Evaluation of the retinal nerve fiber layer in neuromyelitis optica spectrum disorders: a systematic review and meta-analysis. *J Neurol Sci*. 2017;383:108–113. <https://doi.org/10.1016/j.jns.2017.10.028>.
- Tsiligianni I, Kocks J, Tzanakis N, Siafakas N, van der Molen T. Factors that influence disease-specific quality of life or health status in patients with COPD: a review and meta-analysis of Pearson correlations. *Prim Care Respir J: J Gen Pract Airways Group*. 2011;20(3):257–268. <https://doi.org/10.4104/pcrj.2011.00029>.
- Zhang X, Xiao H, Liu C, et al. Comparison of macular structural and vascular changes in neuromyelitis optica spectrum disorder and primary open angle glaucoma: a cross-sectional study. *Br J Ophthalmol*. 2020. <https://doi.org/10.1136/bjophthalmol-2020-315842>.
- Peng C, Li L, Yang M, et al. Different alteration patterns of sub-macular choroidal thicknesses in aquaporin-4 immunoglobulin G antibodies sero-positive neuromyelitis optica spectrum diseases and isolated optic neuritis. *Acta Ophthalmol*. 2020. <https://doi.org/10.1111/aos.14325>.
- Kwapong WR, Yan J, Xie L, et al. Retinal microvasculature alterations in neuromyelitis optica spectrum disorders before optic neuritis. *Mult Scler related Disord*. 2020;44:102277. <https://doi.org/10.1016/j.msard.2020.102277>.
- Chen Y, Shi C, Zhou L, Huang S, Shen M, He Z. The detection of retina microvascular density in subclinical aquaporin-4 antibody seropositive neuromyelitis optica spectrum disorders. *Front Neurol*. 2020;11:35. <https://doi.org/10.3389/fneur.2020.00035>.
- Vabanesi M, Pisa M, Guerrieri S, et al. In vivo structural and functional assessment of optic nerve damage in neuromyelitis optica spectrum disorders and multiple sclerosis. *Sci Rep*. 2019;9(1):10371. <https://doi.org/10.1038/s41598-019-46251-3>.
- Sotirchos ES, Filippatou A, Fitzgerald KC, et al. Aquaporin-4 IgG seropositivity is associated with worse visual outcomes after optic neuritis than MOG-IgG seropositivity and Multiple Sclerosis, independent of macular Ganglion cell layer thinning. *Mult Scler*. 2019. <https://doi.org/10.1177/1352458519864928>. Houndmills, Basingstoke, England.
- Shen T, You Y, Arunachalam S, et al. Differing structural and functional patterns of optic nerve damage in Multiple Sclerosis and neuromyelitis optica spectrum disorder. *Ophthalmology*. 2019;126(3):445–453. <https://doi.org/10.1016/j.ophtha.2018.06.022>.
- Pisa M, Ratti F, Vabanesi M, et al. Subclinical neurodegeneration in Multiple Sclerosis and neuromyelitis optica spectrum disorder revealed by Optical Coherence Tomography. *Mult Scler*. 2019. <https://doi.org/10.1177/1352458519861603>. Houndmills, Basingstoke, England.
- Huang Y, Zhou L, JZhangBao, et al. Peripapillary and parafoveal vascular network assessment by optical coherence tomography angiography in aquaporin-4 antibody-positive neuromyelitis optica spectrum disorders. *Br J Ophthalmol*. 2019;103(6):789–796. <https://doi.org/10.1136/bjophthalmol-2018-312231>.
- Filgueiras TG, Oyama MK, Preti RC, Apóstolos-Pereira SL, Callegaro D, Monteiro MLR. Outer retinal dysfunction on multifocal electroretinography may help differentiating Multiple Sclerosis from neuromyelitis optica spectrum disorder. *Front Neurol*. 2019;10:928. <https://doi.org/10.3389/fneur.2019.00928>.
- Çolpak AI, Sevim DG, Tuncer A, et al. Analysis of peripapillary retinal nerve fiber layer and macular volume in patients with Multiple Sclerosis, neuromyelitis optica spectrum disorders, and healthy controls using spectral domain optical coherence tomography in a Turkish cohort. *Türk Noroloji Dergisi*. 2019;25(1):26–31. <https://doi.org/10.4274/tnd.galenos.2018.33230>.
- Zhao X, Qiu W, Zhang Y, et al. A prospective case-control study comparing optical coherence tomography characteristics in neuromyelitis optica spectrum disorder-optic neuritis and idiopathic optic neuritis. *BMC Ophthalmol*. 2018;18(1):247. <https://doi.org/10.1186/s12886-018-0902-3>.
- Tian DC, Su L, Fan M, et al. Bidirectional degeneration in the visual pathway in neuromyelitis optica spectrum disorder (NMOSD). *Mult Scler*. 2018;24(12):1585–1593. <https://doi.org/10.1177/1352458517727604>.
- Oertel FC, Havla J, Roca-Fernández A, et al. Retinal ganglion cell loss in neuromyelitis optica: a longitudinal study. *J Neurol Neurosurg Psychiatr*. 2018;89(12):1259–1265. <https://doi.org/10.1136/jnnp-2018-318382>.
- Mekhasingharak N, Laowanapibon P, Siritho S, et al. Optical coherence tomography in central nervous system demyelinating diseases related optic neuritis. *Int J Ophthalmol*. 2018;11(10):1649–1656. <https://doi.org/10.18240/ijo.2018.10.12>.
- Kim NH, Kim HJ, Park CY, Jeong KS, JYCho, Lu PR. Retinal ganglion cell-inner plexiform and nerve fiber layers in neuromyelitis optica. *Int J Ophthalmol*. 2018;11(1):89–93. <https://doi.org/10.18240/ijo.2018.01.16>.
- Peng CX, Li HY, Wang W, et al. Retinal segmented layers with strong aquaporin-4 expression suffered more injuries in neuromyelitis optica spectrum disorders compared with optic neuritis with aquaporin-4 antibody seronegativity detected by optical coherence tomography. *Br J Ophthalmol*. 2017;101(8):1032–1037. <https://doi.org/10.1136/bjophthalmol-2016-309412>.
- Matsumoto Y, Mori S, Ueda K, et al. Impact of the anti-aquaporin-4 autoantibody on inner retinal structure, function and structure-function associations in Japanese patients with optic neuritis. *PLoS One*. 2017;12(2), e0171880. <https://doi.org/10.1371/journal.pone.0171880>.
- Peng C, Wang W, Xu Q, et al. Structural alterations of segmented macular inner layers in aquaporin-4-antibody-positive optic neuritis patients in a Chinese population. *PLoS One*. 2016;11(6). <https://doi.org/10.1371/journal.pone.0157645>.
- Pache F, Zimmermann H, Mikolajczak J, et al. MOG-IgG in NMO and related disorders: a multicenter study of 50 patients. Part 4: afferent visual system damage after optic neuritis in MOG-IgG-seropositive versus AQP4-IgG-seropositive patients. *J Neuroinflammation*. 2016;13. <https://doi.org/10.1186/s12974-016-0720-6>.
- Martínez-Lapiscina EH, Sepulveda M, Torres-Torres R, et al. Usefulness of optical coherence tomography to distinguish optic neuritis associated with AQP4 or MOG in neuromyelitis optica spectrum disorders. *Therapeut Adv Neurol Disord*. 2016;9(5):436–440. <https://doi.org/10.1177/1756285616655264>.
- Manogaran P, Vavasour IM, Lange AP, et al. Quantifying visual pathway axonal and myelin loss in Multiple Sclerosis and neuromyelitis optica. *Neuroimage-Clin*. 2016;11:743–750. <https://doi.org/10.1016/j.nicl.2016.05.014>.
- Jeong IH, Kim HJ, Kim NH, Jeong KS, Park CY. Subclinical primary retinal pathology in neuromyelitis optica spectrum disorder. *J Neurol*. 2016;263(7):1343–1348. <https://doi.org/10.1007/s00415-016-8138-8>.
- Cheng L, Wang J, He X, Xu X, Ling ZF. Macular changes of neuromyelitis optica through spectral-domain optical coherence tomography. *Int J Ophthalmol*. 2016;9(11):1638–1645. <https://doi.org/10.18240/ijo.2016.11.17>.
- Park KA, Kim J, Oh SY. Analysis of spectral domain optical coherence tomography measurements in optic neuritis: differences in neuromyelitis optica, Multiple Sclerosis, isolated optic neuritis and normal healthy controls. *Acta Ophthalmol*. 2014;92(1):e57–65. <https://doi.org/10.1111/aos.12215>.
- Sotirchos ES, Saidha S, Byraiah G, et al. In vivo identification of morphologic retinal abnormalities in neuromyelitis optica. *Neurology*. 2013;80(15):1406–1414. <https://doi.org/10.1212/WNL.0b013e31828c2f7a>.
- Schneider E, Zimmermann H, Oberwahrenbrock T, et al. Optical coherence tomography reveals distinct patterns of retinal damage in neuromyelitis optica and Multiple Sclerosis. *PLoS One*. 2013;8(6), e66151. <https://doi.org/10.1371/journal.pone.0066151>.
- Lange AP, Sadjadi R, Zhu F, Alkairie S, Costello F, Traboulsi AL. Spectral-domain optical coherence tomography of retinal nerve fiber layer thickness in NMO patients. *J Neuro Ophthalmol: Off J North Am Neuro-Ophthalmol Soc*. 2013;33(3):213–219. <https://doi.org/10.1097/WNO.0b013e31828c5f0e>.
- Hokazono K, Raza AS, Oyama MK, Hood DC, Monteiro ML. Pattern electroretinogram in neuromyelitis optica and Multiple Sclerosis with or without optic neuritis and its correlation with FD-OCT and perimetry, Documenta

- ophthalmologica. *Adv Ophthalmol*. 2013;127(3):201–215. <https://doi.org/10.1007/s10633-013-9401-2>.
38. Syc SB, Saidha S, Newsome SD, et al. Optical coherence tomography segmentation reveals ganglion cell layer pathology after optic neuritis. *Brain : J Neurol*. 2012; 135(Pt 2):521–533. <https://doi.org/10.1093/brain/awr264>.
 39. Monteiro ML, Fernandes DB, Apóstolos-Pereira SL, Callegaro D. Quantification of retinal neural loss in patients with neuromyelitis optica and Multiple Sclerosis with or without optic neuritis using Fourier-domain optical coherence tomography. *Investig Ophthalmol Vis Sci*. 2012;53(7):3959–3966. <https://doi.org/10.1167/iov.11-9324>.
 40. Nakamura M, Nakazawa T, Doi H, et al. Early high-dose intravenous methylprednisolone is effective in preserving retinal nerve fiber layer thickness in patients with neuromyelitis optica. *Graefes Arch Clin Exp Ophthalmol = Albrecht von Graefes Archiv für klinische und experimentelle Ophthalmologie*. 2010;248(12): 1777–1785. <https://doi.org/10.1007/s00417-010-1344-7>.
 41. Ratchford JN, Quigg ME, Conger A, et al. Optical coherence tomography helps differentiate neuromyelitis optica and MS optic neuropathies. *Neurology*. 2009;73(4): 302–308. <https://doi.org/10.1212/WNL.0b013e3181af78b8>.
 42. Naismith RT, Tutlam NT, Xu J, et al. Optical coherence tomography differs in neuromyelitis optica compared with Multiple Sclerosis. *Neurology*. 2009;72(12): 1077–1082. <https://doi.org/10.1212/01.wnl.0000345042.53843.d5>.
 43. Green AJ, Cree BA. Distinctive retinal nerve fibre layer and vascular changes in neuromyelitis optica following optic neuritis. *J Neurol Neurosurg Psychiatr*. 2009; 80(9):1002–1005. <https://doi.org/10.1136/jnnp.2008.166207>.
 44. Zeng P, Du C, Zhang R, et al. Optical coherence tomography reveals longitudinal changes in retinal damage under different treatments for neuromyelitis optica spectrum disorder. *Front Neurol*. 2021;12. <https://doi.org/10.3389/fneur.2021.669567>.
 45. Yu J, Wong W, Quan C, Wang M. The characteristics of optical coherence tomography angiography in aquaporin-4 antibody positive neuromyelitis optica spectrum disorders. *Chin J Ocular Fundus Dis*. 2021;37(3):173–179. <https://doi.org/10.3760/cma.j.cn511434-20200429-00189>.
 46. Yu J, Huang Y, Zhou L, et al. Comparison of the retinal vascular network and structure in patients with optic neuritis associated with myelin oligodendrocyte glycoprotein or aquaporin-4 antibodies: an optical coherence tomography angiography study. *J Neurol*. 2021. <https://doi.org/10.1007/s00415-021-10609-3>.
 47. Rogaczewska M, Michalak S, Stopa M. Optical coherence tomography angiography of peripapillary vessel density in Multiple Sclerosis and neuromyelitis optica spectrum disorder: a comparative study. *J Clin Med*. 2021;10(4). <https://doi.org/10.3390/jcm10040609>.
 48. Roca-Fernández A, Oertel FC, Yeo T, et al. Foveal changes in aquaporin-4 antibody seropositive neuromyelitis optica spectrum disorder are independent of optic neuritis and not overtly progressive. *Eur J Neurol*. 2021;28(7):2280–2293. <https://doi.org/10.1111/ene.14766>.
 49. AbdulRasool S, Abbas KO, Rasheed AAR. Estimation of peripapillary retinal nerve fibre layer thickness in neuromyelitisoptica spectrum disorders and relapse-remitting Multiple Sclerosis by optical coherence tomography in Iraqi people. *Ann Trop Med Publ Health*. 2020;23(13). <https://doi.org/10.36295/ASRO.2020.231376>.
 50. Ringelstein M, Harmel J, Zimmermann H, et al. Longitudinal optic neuritis-unrelated visual evoked potential changes in NMO spectrum disorders. *Neurology*. 2020;94(4): e407–e418. <https://doi.org/10.1212/WNL.0000000000008684>.
 51. Jeong IH, Choi JY, Kim SH, et al. Normal-appearing white matter demyelination in neuromyelitis optica spectrum disorder. *Eur J Neurol*. 2017;24(4):652–658. <https://doi.org/10.1111/ene.13266>.
 52. Ventura RE, Kister I, Chung S, Babb JS, Shepherd TM. Cervical spinal cord atrophy in NMOSD without a history of myelitis or MRI-visible lesions. *Neurol(R) Neuroimmunol Neuroinflammation*. 2016;3(3):e224. <https://doi.org/10.1212/NXI.0000000000000224>.
 53. Chen T, Lennon VA, Liu YU, et al. Astrocyte-microglia interaction drives evolving neuromyelitis optica lesion. *J Clin Invest*. 2020;130(8):4025–4038. <https://doi.org/10.1172/JCI134816>.
 54. Petzold A, Balcer LJ, Calabresi PA, et al. Retinal layer segmentation in Multiple Sclerosis: a systematic review and meta-analysis. *Lancet Neurol*. 2017;16(10): 797–812. [https://doi.org/10.1016/S1474-4422\(17\)30278-8](https://doi.org/10.1016/S1474-4422(17)30278-8).
 55. Oertel FC, Zimmermann H, Paul F, Brandt AU. Optical coherence tomography in neuromyelitis optica spectrum disorders: potential advantages for individualized monitoring of progression and therapy. *EPMA J*. 2018;9(1):21–33. <https://doi.org/10.1007/s13167-017-0123-5>.
 56. Oertel FC, Kuchling J, Zimmermann H, et al. Microstructural visual system changes in AQP4-antibody-seropositive NMOSD. *Neurol(R) Neuroimmunol Neuroinflammation*. 2017;4(3):e334. <https://doi.org/10.1212/NXI.0000000000000334>.
 57. Havla J, Kümpfel T, Schinner R, et al. Myelin-oligodendrocyte-glycoprotein (MOG) autoantibodies as potential markers of severe optic neuritis and subclinical retinal axonal degeneration. *J Neurol*. 2017;264(1):139–151. <https://doi.org/10.1007/s00415-016-8333-7>.
 58. Pache F, Zimmermann H, Mikolajczak J, et al. In NMO and related disorders: a multicenter study of 50 patients. Part 4: afferent visual system damage after optic neuritis in MOG-IgG-seropositive versus AQP4-IgG-seropositive patients. *J Neuroinflammation*. 2016;13(1):282. <https://doi.org/10.1186/s12974-016-0720-6>.
 59. Outteryck O, Majeed B, Defoort-Dhellemmes S, Vermersch P, Zéphir H. A comparative optical coherence tomography study in neuromyelitis optica spectrum disorder and Multiple Sclerosis. *Mult Scler*. 2015;21(14):1781–1793. <https://doi.org/10.1177/1352458515578888>.
 60. von Glehn F, Jarius S, Cavalcanti Lira RP, et al. Structural brain abnormalities are related to retinal nerve fiber layer thinning and disease duration in neuromyelitis optica spectrum disorders. *Mult Scler*. 2014;20(9):1189–1197. <https://doi.org/10.1177/1352458513519838>.
 61. Fernandes DB, Raza AS, Nogueira RG, et al. Evaluation of inner retinal layers in patients with Multiple Sclerosis or neuromyelitis optica using optical coherence tomography. *Ophthalmology*. 2013;120(2):387–394. <https://doi.org/10.1016/j.ophtha.2012.07.066>.